Inorg. Chem. **2000,** *39,* 2397−2404 **2397**

Syntheses, Structures, and Fluxionality of Blue Luminescent Zinc(II) Complexes: Zn(2,2′,2″-tpa)Cl$_2$, Zn(2,2′,2″-tpa)$_2$(O$_2$CCF$_3$)$_2$, and Zn(2,2′,3″-tpa)$_4$(O$_2$CCF$_3$)$_2$ (tpa = Tripyridylamine)

Wenyu Yang, Hartmut Schmider, Qingguo Wu, You-sheng Zhang, and Suning Wang*

Department of Chemistry, Queen's University, Kingston, Ontario K7L 3N6, Canada

Received December 16, 1999

Three novel Zn(II) complexes containing either 2,2′,2″-tripyridylamine (2,2′,2″-tpa) or 2,2′,3″-tripyridylamine (2,2′,3″-tpa) have been synthesized and structurally characterized. Compound **1**, Zn(2,2′,2″-tpa)Cl$_2$, has a tetrahedral geometry while compounds **2**, Zn(2,2′,2″-tpa)$_2$(O$_2$CCF$_3$)$_2$, and **3**, Zn(2,2′,3″-tpa)$_4$(O$_2$CCF$_3$)$_2$, have an octahedral geometry. The 2,2′,2″-tpa ligand in **1** and **2** functions as a bidentate ligand, chelating to the zinc center, while the 2,2″,3″-tpa ligand in **3** functions as a terminal ligand, binding to the zinc center through the 3-pyridyl nitrogen atom. All three compounds emit a blue color in solution and in the solid state. The emission maxima for the three compounds in solution are at $\lambda = 422$, 426, and 432 nm, respectively. The blue luminescence of the complexes is due to a $\pi^* \rightarrow \pi$ transition of the tpa ligand as established by an ab initio calculation on the free ligand 2,2′,2″-tpa and complex **1**. Compounds **1** and **2** are fluxional in solution owing to an exchange process between the coordinate and noncoordinate 2-pyridyl rings of the 2,2′,2″-tpa ligand. Compound **2** is also fluxional owing to a cis−trans isomerization process, as determined by variable-temperature ^{1}H NMR spectroscopic analysis.

Introduction

Luminescent organic and coordination compounds have been an active research area for decades because of their various potential applications in materials sciences. The most notable recent interest in luminescent compounds concerns their applications in electroluminescent displays.[1−3] In electroluminescence, electrical energy is converted to light via a medium of luminescent materials.[1] Electroluminescent devices using various compounds including organic polymers, small organic molecules, and coordination compounds have been fabricated successfully either by a spin-coating or a vacuum sublimation process. To achieve full-color electroluminescent displays, three color components, i.e., green, blue, and red, must be available. Stable blue luminescent compounds that are useful in electroluminescent devices are still rare and very challenging to prepare. We have demonstrated that 7-azaindole or 2,2′-dipyridylamine can produce a bright blue luminescence when deprotonated and bound to either an aluminum ion or a boron center.[4] Blue electroluminescent devices using 7-azaindole−boron compounds have been fabricated successfully.[3f] However, many of our previously reported aluminum or boron compounds based on 7-azaindole or 2,2′-dipyridylamine are not stable enough for electroluminescent devices. The instability of these compounds is due mostly to the fact that 7-azaindole or 2,2′-dipyridylamine in the complexes is negatively charged and hence susceptible to moisture in air. Our recent efforts have therefore focused on (1) stabilizing the charge on the negatively charged ligand and (2) using neutral ligands. In this paper, we report the results of our investigation on blue luminescent zinc(II) complexes using neutral 2,2′,2″-tripyridylamine (2,2′,2″-tpa) and 2,2′,3″-tripyridylamine (2,2′,3″-tpa) as the light-emitting ligands.

Experimental Section

All reactions were carried out under a nitrogen atmosphere. All starting materials were purchased from Aldrich Chemical Co. and used without further purification, unless otherwise stated. Tetrahydrofurnan, hexane, and toluene were distilled from sodium and benzophenone under a nitrogen atmosphere, and dichloromethane was distilled from P$_2$O$_5$ under a nitrogen atmosphere. ^{1}H NMR spectra were recorded on Bruker Avance 300 and 400 MHz spectrometers. The Canadian Microanalytical Service Ltd., Delta, British Columbia, performed the elemental analyses. TLC was also carried out on SiO$_2$ (silica gel F254, Whatman), and column chromatography was also carried out on silica (silica gel 60, 70−230 mesh). Melting points were determined on a Fisher-Johns melting point apparatus, and excitation and emission spectra were recorded on a Photon Technologies International QuantaMaster model C-60 spectrometer.

---

(1) (a) Tang, C. W.; VanSlyke, S. A. *Appl. Phys. Lett.* **1987**, *51*, 913. (b) Tang, C. W.; VanSlyke, S. A.; Chen, C. H. *J. Appl. Phys.* **1989**, *65*, 3611. (c) Shirota, Y.; Kuwabara, Y.; Inada, H.; Wakimoto, T.; Nakada, H.; Yonemoto, Y.; Kawami, S.; Imai, K. *Appl. Phys. Lett.* **1994**, *65*, 807. (d) Hamada, Y.; Sano, T.; Fujita, M.; Fujii, T.; Nishio, Y.; Shibata, K. *Jpn. J. Appl. Phys.* **1993**, *32*, L514. (e) Bulovic, V.; Gu, G.; Burrows, P. E.; Forrest, S. R. *Nature* **1996**, *380*, 29.

(2) (a) Adachi, C.; Tokito, S.; Tsutsui, T.; Saito, S. *Jpn. J. Appl. Phys.* **1988**, *27*, L713. (b) Adachi, C.; Tsutsui, T.; Saito, S. *Appl. Phys. Lett.* **1990**, *56*, 799. (c) Tao, X. T.; Suzuki, H.; Wada, T.; Sasabe, H.; Miyata, S. *Appl. Phys. Lett.* **1999**, *75*, 1655. (d) Shen, Z.; Burrows, P. E.; Bulovic, V.; Borrest, S. R.; Thompson, M. E. *Science* **1997**, *276*, 2009. (e) Aziz, H.; Popovic, Z. D.; Hu, N.-X.; Hor, A.-M.; Xu, G. *Science* **1999**, *283*, 1900.

(3) (a) Hu, N.-X.; Esteghamatian, M.; Xie, S.; Popovic, P.; Ong, B.; Hor, A.-M.; Wang, S. *Adv. Mater.* **1999**, *11*, 1460. (b) Hamada, Y.; Sano, T.; Fujii, H.; Nishio, Y.; Takahashi, H.; Shibata, K. *Appl. Phys. Lett.* **1997**, *71*, 3338. (c) Hamada, Y.; Sano, T.; Fujita, M.; Fujii, T.; Nishio, Y.; Shibata, K. *Chem. Lett.* **1993**, 905. (d) Baldo, M. A.; Lamansky, S.; Burrows, P.; Thompson, M. E.; Forrest, S. R. *Appl. Phys. Lett.* **1999**, *75*, 5. (e) Wu, Q.; Esteghamatian, M.; Hu, N.-X.; Popovic, Z.; Enright, G.; Tao, Y.; D'Iorio, M.; Wang, S. *Chem. Mater.*, in press. (f) Wu, Q.; Esteghamatian, M.; Hu, N.-X.; Popovic, Z. D.; Enright, G.; Breeze, S. R.; Wang, S. *Angew. Chem., Int. Ed. Engl.* **1999**, *38*, 985.

(4) (a) Hassan, A.; Wang, S. *J. Chem. Soc. Chem. Commun.* **1998**, 211. (b) Liu, W.; Hassan, A.; Wang, S. *Organometallics* **1997**, *16*, 4257. (c) Ashenhurst, J.; Brancaleon, L.; Hassan, A.; Liu, W.; Schmider, H.; Wang, S.; Wu, Q. *Organometallics* **1998**, *17*, 3186−3195. (d) Hassan, A.; Wang, S., *J. Chem. Soc., Chem. Commun.* **1998**, 339.

10.1021/ic991436m CCC: $19.00

Synthesis of Zn(CF$_3$COO)$_2$. A 2.70 g (0.033 mol) sample of ZnO was placed in a 100 mL flask, and 15.00 g of CF$_3$COOH (excess) was added. The mixture was stirred for 2 h at ambient temperature. After all ZnO reacted with CF$_3$COOH, excess CF$_3$COOH was removed under vacuum. The product was washed with diethyl ether and dried in a vacuum at 50 °C overnight, giving 9.30 g (0.032 mmol) of Zn(CF$_3$COO)$_2$ (98% yield).

Synthesis of 2,2′,2″-Tripyridylamine (2,2′,2″-tpa). A 4.00 g (0.023 mol) sample of 2,2′-dipyridylamine, 5.54 g (0.035 mol) of 2-bromopyridine, 2.08 g (0.037 mol) of potassium hydroxide, and 120 mg of cupric sulfate (catalyst) were placed in a 100 mL flask. The mixture was heated to 180 °C and stirred for 6 h. The reaction was monitored by TLC. After the reaction mixture was cooled to ambient temperature, dichloromethane and water were added to dissolve the solids. The aqueous phase was discarded, and the organic phase was washed with distilled water until the pH was 7. Na$_2$SO$_4$ was used to dry the organic phase. The product was isolated by using a chromatographic column with ethanol as the eluant. Colorless crystals of 2,2′,2″-tpa were obtained in 48% yield from an ethanol/hexane solution. Mp: 129−131 °C. ^{1}H NMR (δ, ppm; CDCl$_3$, 298 K): 8.43 (1H, d, $^3J = 5.1$ Hz), 7.68 (1H, dd, $^3J = 7.5$ Hz), 7.11 (1H, d, $^3J = 6.9$ Hz), 7.08 (1H, dd, $^3J = 5.1$ Hz)

Synthesis of 2,2′,3″-Tripyridylamine (2,2′,3″-tpa). A 3.03 g (0.018 mol) sample of 2,2′-dipyridylamine, 3.08 g (0.019 mol) of 3-bromopyridine, 1.40 g (0.025 mol) of potassium hydroxide, and 0.075 g of cupric sulfate (catalyst) were placed in a 100 mL flask. The mixture was heated to 180 °C and stirred for 5 h. After the reaction mixture was cooled to ambient temperature, dichoromethane and water were added to dissolve the solids. The aqueous phase was discarded. The organic phase was washed with distilled water until the pH was 7 and dried over Na$_2$SO$_4$. The product was isolated by using a chromatographic column and a mixed-solvent eluant (ethyl acetate/ethanol, 1:1). Colorless crystals of 2,2′,3″-tripyridylamine were obtained in 57% yield from a solution of ethanol/ethyl acetate/hexane. Mp: 103−105 °C. ^{1}H NMR (δ, ppm; CDCl$_3$, 298 K): 8.35 (2H, d, $^3J = 4.8$ Hz), 8.46 (1H, s), 8.44 (2H, d, $^3J = 4.8$ Hz), 7.63 (2H, dd, $^3J_1 = 8.4$ Hz, $^3J_2 = 7.2$ Hz), 7.55 (1H, d, $^3J = 8.1$ Hz), 7.34 (1H, dd, $^3J_1 = 8.1$ Hz, $^3J_2 = 4.8$ Hz), 7.04 (2H, d, $^3J = 8.4$ Hz), 7.01 (1H, dd, $^3J_1 = 7.2$ Hz, $^3J_2 = 4.8$ Hz).

Synthesis of Zn(2,2′,2″-tpa)Cl$_2$ (1). A 55 mg (0.40 mmol) quantity of ZnCl$_2$ was dissolved in methanol. A 100 mg (0.40 mmol) sample of 2,2′,2″-tpa in dissolved in methanol was then added to the ZnCl$_2$ solution at ambient temperature. Colorless solids appeared at once. Colorless crystals of **1** (71 mg, 0.19 mmol) were obtained in 46% yield by recrystallization from chloroform and hexane. Mp: 265−267 °C. ^{1}H NMR (δ, ppm; CDCl$_3$, 298 K): 8.64 (1H, d, $^3J = 5.4$ Hz), 7.90 (1H, dd, $^3J_1 = 8.4$ Hz, $^3J_2 = 5.1$ Hz), 7.62 (1H, d, $^3J = 8.4$ Hz), 7.39 (1H, dd, $^3J_1 = 5.1$ Hz, $^3J_2 = 5.4$ Hz). Anal. Calcd for C$_{15}$H$_{12}$N$_4$ZnCl$_2$: C, 46.85; H, 3.15; N, 14.57. Found: C, 46.55; H, 3.18; N, 14.51.

Synthesis of Zn(2,2′,2″-tpa)$_2$(CF$_3$COO)$_2$ (2). A 200 mg quantity of Zn(CF$_3$COO)$_2$ (0.69 mmol) and 343 mg of 2,2′,2″-tpa (1.38 mmol) were dissolved in THF, and the mixture was stirred for 1 h at ambient temperature. After concentration of the solution, a small amount of hexane was added. Colorless crystals of **2** were obtained in 84% yield. Mp: 179−180 °C. ^{1}H NMR (δ, ppm; CDCl$_3$, 298 K): 8.57 (1H, d, $^3J = 3.9$ Hz), 7.78 (1H, dd, $^3J_1 = 8.4$ Hz $^3J_2 = 7.2$ Hz), 7.11 (1H, d, $^3J = 8.4$ Hz), 7.08 (1H, dd, $^3J = 7.2$ Hz). Anal. Calcd for Zn(CF$_3$COO)$_2$(2,2′,2″-tpa)$_2$: C, 51.82; N, 14.22; H, 3.07. Found: C, 51.73; N, 14.27; H, 3.08.

Synthesis of Zn(2,2′,3″-tpa)$_4$(CF$_3$COO)$_2$ (3). A 29 mg (0.10 mmol) quantity of Zn(CF$_3$COO)$_2$ and 99 mg (0.40 mmol) of 2,2′,3″-tpa were dissolved in THF, and the mixture was stirred for 1 h at ambient temperature. After concentration of the solution and the addition of a small amount of hexane, colorless crystals of compound **3** were obtained in 77% yield. Mp: 112−114 °C. ^{1}H NMR (δ, ppm; CDCl$_3$, 298 K): 8.56 (1H, s), 8.50 (1H, br), 8.39 (2H, d, $^3J = 3.9$ Hz), 7.76 (1H, d, $^3J = 8.4$ Hz), 7.69 (2H, dd, $^3J = 7.2$ Hz), 7.48 (1H, dd, $^3J = 7.5$ Hz), 7.10 (2H, dd, $^3J_1 = 7.2$ Hz, $^3J_2 = 3.9$ Hz), 7.05 (2H, d, $^3J = 7.2$ Hz). Anal. Calcd for Zn(CF$_3$COO)$_2$(2,2′,3″-tpa)$_4$: C, 59.84; H, 3.77; N, 17.45. Found: C, 60.26; H, 3.86; N, 16.76.

X-ray Crystallographic Analysis. All crystals were obtained either from CH$_2$Cl$_2$/hexane solutions or from THF/hexane solutions and were mounted on glass fibers. All data were collected on a Siemens P4 single-crystal diffractometer with graphite-monochromated Mo Kα radiation, operating at 50 kV and 35 mA at 23 °C. The data for **1**−**3** were collected over 2θ ranges of 3−47, 3−50, and 3−45°, respectively. The data for 2,2′,2″-tpa and 2,2′,3″-tpa were collected over 2θ ranges of 3−68 and 3−45°, respectively. Three standard reflections were measured every 197 reflections. No significant decay was observed for any of the samples. Data were processed on a Pentium PC using the Siemens SHELXTL software package[5] (version 5.0) and corrected for absorption, Lorentz, and polarization effects. Neutral-atom scattering factors were taken from Cromer and Waber.[6] The crystals of **1**, **2**, and 2,2′,3″-tpa belong to the monoclinic space groups $P2_1/c$, $P2/c$, and $P2_1/n$, respectively, uniquely determined by systematic absences. The crystal of **3** belongs to the triclinic space group $P\bar{1}$, while the crystals of 2,2′,2″-tpa belong to the rhombohedral space group $R3$. All structures were solved by direct methods. Some of the CF$_3$ groups in compounds **2** and **3** display a typical 2-fold rotational disorder, which was modeled and refined successfully. All non-hydrogen atoms were refined anisotropically, except those of some of the disordered CF$_3$ groups. The positions for all hydrogen atoms in compounds **1**−**3** were calculated, and their contributions were included in the structure factor calculations. All hydrogen atoms in the free ligands were located directly from difference Fourier maps and refined successfully. The crystallographic data for compounds **1**−**3** and the ligands are given in Table 1.

Results and Discussion

Syntheses and Crystal Structures. (a) Ligands. 2,2′-Dipyridylamine has no emission in the visible region. When it is coordinated to a metal center such as Zn(II) or Al(III) as a neutral ligand, weak emission at $\lambda_{\max} < 400$ nm is observed.[7] The near-UV emission makes 2,2′-dipyridylamine complexes unsuitable as blue emitters for electroluminescent applications. Aluminum or boron complexes with deprotonated 2,2′-dipyridylamine, albeit producing bright blue emission at ∼470 nm, are in general too unstable to be useful in electroluminescent devices.[4] Because the HOMO−LUMO gap of the ligand can be affected by substituents, complexes containing properly modified 2,2′-dipyridylamine may have an emission in the blue region with an improved efficiency. We therefore carried out the syntheses of modified 2,2′-dipyridylamine (dpa) ligands by replacing the proton on the nitrogen atom of dpa with an aliphatic or aromatic group R. Among the new modified dpa ligands, only 2,2′,2″-tripyridylamine (2,2′,2″-tpa) and 2,2′,3″-tripyridylamine (2,2′,3″-tpa) yield blue luminescence when coodinated to an Al(III) ora Zn(II) ion. Therefore, our investigation focused on these two ligands. The syntheses of these two ligands were carried out by using Ullmann condensation methods,[8] where copper(II) and KOH are used as catalysts (Scheme 1).

The structures of both ligands were examined by a single-crystal X-ray diffraction analysis. As shown in Figure 1, the 2,2′,2″-tpa ligand is nonplanar and has a crystallographically imposed C_3 symmetry. The central nitrogen atom N(1) is coplanar with the three carbon atoms to which it binds (the maximum deviation of the nitrogen atom from the NC$_3$ plane is 0.028 Å), while the three pyridyl rings have a propeller arrangement with a dihedral angle of 35.3° between the central

---

(5) *SHELXTL: crystal structure analysis package*, Version 5; Siemens: Madison, WI, 1995.

(6) Cromer, D. T.; Waber, J. T. *International Tables for X-ray Crystallography*; Kynoch Press: Birmingham, U.K., 1974; Vol. 4, Table 2.2A.

(7) (a) Ho, K. Y.; Yu, W. Y.; Cheung, K. K.; Che, C. M., *J. Chem. Soc., Chem. Commun.* **1998**, 2101. (b) Ho, K. Y.; Yu, W. Y.; Cheung, K. K.; Che, C. M. *J. Chem. Soc., Dalton Trans.* **1999**, 1581.

(8) (a) Goodbrand, H. B.; Hu, N. X. *J. Org. Chem.*, **1999**, *64*, 670. (b) Lindley, J. *Tetrahedron* **1984**, *40*, 1433. (c) Fanta, P. E. *Synthesis* **1974**, 1.

Table 1. Crystallographic Data for the Ligands and Compounds **1**−**3**

	2,2′,2″-tpa	2,2′,3″-tpa	**1**	**2**	**3**
formula	$C_{15}H_{12}N_4$	$C_{15}H_{12}N_4$	$C_{15}H_{12}N_4Cl_2Zn$	$C_{34}H_{24}N_4F_6O_4Zn$	$C_{64}H_{48}N_{16}F_6O_4Zn$
fw	248.3	248.3	384.3	787.98	1284.5
space group	*R*3	$P2_1/n$	$P2_1/c$	$P2/c$	$P\bar{1}$
a/Å	15.912(2)	8.758(12)	13.939(2)	19.292(10)	10.222(7)
b/Å	15.912(2)	11.598(6)	8.437(3)	10.466(2)	12.375(3)
c/Å	4.134(1)	24.985(12)	14.193(3)	18.574(4)	13.744(7)
α/deg	90	90	90	90	105.13(5)
β/deg	90	94.72(5)	103.96(1)	113.709(18)	108.34(5)
γ/deg	120	90	90	90	105.50(3)
V/Å^3	906.5(5)	2529(4)	1619.9(7)	3434(2)	1472.7(13)
Z	3	8	4	4	1
D_c/g cm^{-3}	1.364	1.304	1.577	1.524	1.448
μ/cm^{-1}	0.86	0.82	18.46	7.99	5.01
2θ	68	45	47	50	45
λ/Å	0.710 73	0.710 73	0.710 73	0.710 73	0.710 74
temp/°C	23	23	23	23	23
no. of reflns measd	447	3581	2514	6114	3870
no. of reflns used (R_{int})	372 (0.092)	3326 (0.030)	2404 (0.021)	5909 (0.035	3756 (0.040)
no. of variables	74	439	199	503	409
final R values [$I > 2\sigma(I)$]: R1,[a]wR2[b]	0.0685, 0.1293	0.0608, 0.1417	0.0470, 0.1132	0.0737, 0.1858	0.0806, 0.1529
R values (all data): R1,[a] wR2[b]	0.0688, 0.1296	0.1036, 0.1739	0.0675, 0.1244	0.1425, 0.2364	0.1732, 0.1927
goodness-of-fit on F^2	1.326	1.027	1.069	1.058	1.036

[a] $R1 = \sum|F_o| - |F_c|/\sum|F_o|$. [b] $wR2 = [\sum w(f_o^2 - F_c^2)^2/\sum w(F_o^2)^2]^{1/2}$; $w = 1/[\sigma^2(F_o^2) + (0.075P)^2]$, where $P = [\mathrm{Max}(F_o^2, 0) + 2F_c^2]/3$.

Scheme 1

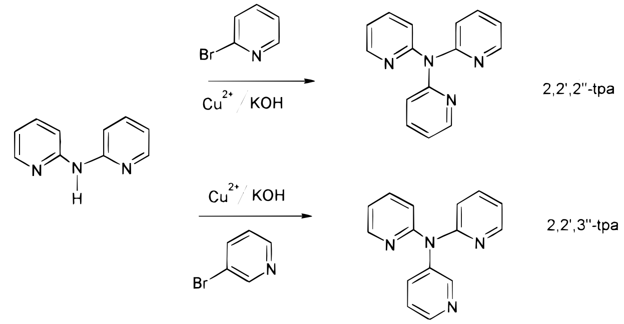

NC$_3$ plane and the pyridyl plane, attributable to steric interactions between the pyridyl rings. All molecules of 2,2′,2″-tpa are stacked along the unique *c* axis with an intermolecular separation distance of 4.134(1) Å. In contrast, 2,2′,3″-tpa crystallizes in the monoclinic crystal system. There are more than one stacking directions for the molecules of 2,2′,3″-tpa in the crystal lattice. Two independent molecules of 2,2′,3″-tpa are present in the asymmetric unit. Both molecules are nonplanar, as is the case for 2,2′,2″-tpa. The central NC$_3$ portion is planar, with a maximum deviation from the NC$_3$ plane of 0.013 Å. The dihedral angles between the pyridyl ring and the NC$_3$ plane in 2,2′,3″-tpa vary from 27.6 to 60.2°, with an average of 38.6°, significantly larger than those in 2,2′,2″-tpa. The presence of a hydrogen atom at the 2- and 6-positions in the 3-pyridyl ring likely increases the steric interaction, leading to an increase in the dihedral angle in comparison to that of 2,2′,2″-tpa. The structure for one of the 2,2′,3″-tpa molecules in the asymmetric unit is shown in Figure 2.

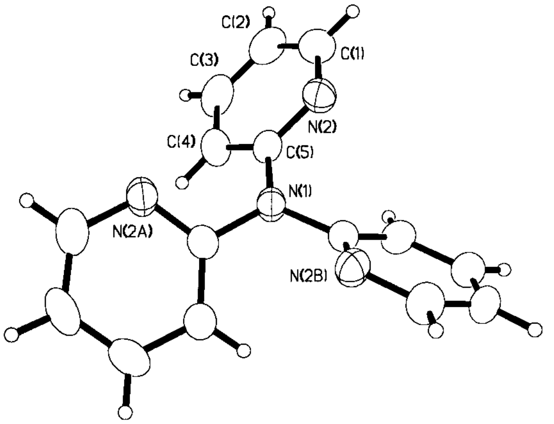

Figure 1. ORTEP diagram showing the structure of the 2,2′,2″-tpa ligand with 50% thermal ellipsoids and the atom-labeling scheme.

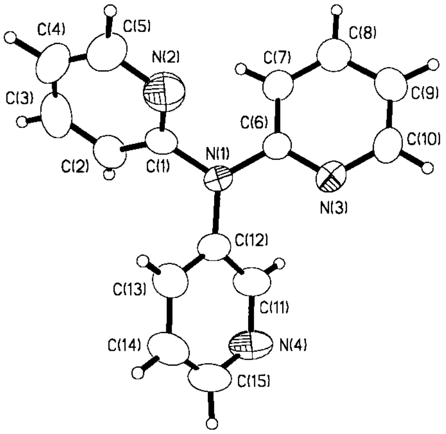

Figure 2. ORTEP diagram showing the structure of the 2,2′,3″-tpa ligand with 50% thermal ellipsoids and the atom-labeling scheme.

Complexes. 2,2′,2″-tpa and 2,2,′3″-tpa ligands react readily with a variety of Zn(II) compounds to form various complexes. Three examples of Zn(II) complexes with these two ligands are presented herein. They are Zn(2,2′,2″-tpa)Cl$_2$ (**1**), obtained from the reaction of 2,2′,2″-tpa with ZnCl$_2$ in a 1:1 ratio, Zn(2,2′,2″-tpa)$_2$(O$_2$CCF$_3$)$_2$ (**2**), obtained from the reaction of 2,2′,2″-tpa with Zn(O$_2$CCF$_3$)$_2$ in a 2:1 ratio, and Zn(2,2′,3″-tpa)$_4$(O$_2$CCF$_3$)$_2$ (**3**), obtained from the reaction of 2,2′,3″-tpa with Zn(O$_2$CCF$_3$)$_2$ in a 4:1 ratio. All three compounds are air stable. The structures of all three compounds weer determined by single-crystal X-ray diffraction analyses. Important bond lengths and angles are listed in Table 2.

Table 2. Selected Bond Lengths (Å) and Angles (deg) for Compounds **1**−**3**

Compound **1**			
Zn(1)−N(1)	2.057(4)	Zn(1)−Cl(2)	2.2011(15)
Zn(1)−N(2)	2.058(4)	Zn(1)−Cl(1)	2.2076(16)
N(1)−Zn(1)−N(2)	88.39(14)	N(1)−Zn(1)−Cl(1)	110.58(12)
N(1)−Zn(1)−Cl(2)	111.91(11)	N(2)−Zn(1)−Cl(1)	110.64(11)
N(2)−Zn(1)−Cl(2)	111.96(11)	Cl(2)−Zn(1)−Cl(1)	119.20(6)
Compound **2**			
Zn(1)−O(1)	2.127(5)	Zn(2)−O(3)	2.110(5)
Zn(1)−N(2)	2.167(6)	Zn(2)−N(5)	2.156(6)
Zn(1)−N(1)	2.167(7)	Zn(2)−N(6)	2.182(5)
O(1)−Zn(1)−O(1A)	87.0(3)	O(3)−Zn(2)−O(3A)	83.9(3)
O(1)−Zn(1)−N(2)	175.0(2)	O(3)−Zn(2)−N(5)	93.7(2)
O(1A)−Zn(1)−N(2)	91.3(2)	O(3A)−Zn(2)−N(5)	86.8(2)
N(2)−Zn(1)−N(2A)	90.8(3)	N(5A)−Zn(2)−N(5)	179.2(3)
O(1)−Zn(1)−N(1)	88.5(3)	O(3)−Zn(2)−N(6)	175.7(2)
O(1A)−Zn(1)−N(1)	90.4(3)	N(5A)−Zn(2)−N(6)	94.9(2)
N(2)−Zn(1)−N(1)	86.9(2)	N(5)−Zn(2)−N(6)	84.6(2)
N(2A)−Zn(1)−N(1)	94.2(2)	O(3)−Zn(2)−N(6A)	92.05(19)
N(1)−Zn(1)−N(1A)	178.4(3)		
Compound **3**			
Zn(1)−O(1)	2.131(6)	Zn(1)−N(1)	2.138(6)
Zn(1)−N(5)	2.270(7)		
O(1)−Zn(1)−O(1A)	180.000(1)	O(1)−Zn(1)−N(5)	93.9(3)
O(1)−Zn(1)−N(1)	92.6(2)	O(1A)−Zn(1)−N(5)	86.1(3)
O(1)−Zn(1)−N(1A)	87.4(2)	N(1)−Zn(1)−N5)	89.8(2)
N(1)−Zn(1)−N(1A)	180.000(2)	N(5A)−Zn(1)−N(5)	180.000(1)
N(1)−Zn(1)−N(5A)	90.2(2)		

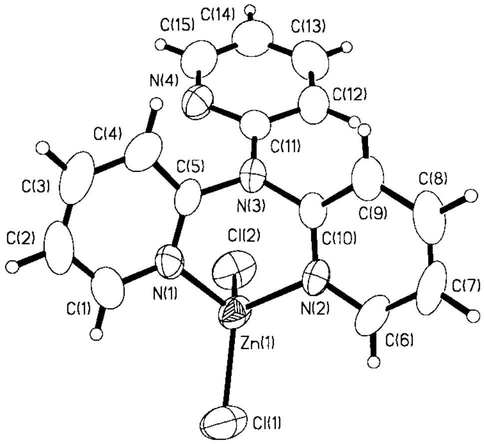

Figure 3. ORTEP diagram showing the structure of compound **1** with 50% thermal ellipsoids and the atom-labeling scheme.

As shown in Figure 3, two of the 2-pyridyl rings in 2,2′,2″-tpa chelate to the Zn(II) center in compound **1**. The N(1)−Zn(1)−N(2) angle of 88.39(14)° is much less than a typical tetrahedral bond angle (109°). Compound **1** is therefore a somewhat distorted tetrahedron. The amino nitrogen atom N(3) is coplanar with the three carbon atoms to which it binds (C(5), C(10), and C(11); the sum of bond angles around N(3) is 360°), as in the free ligand. One of the pyridyl rings (N(4)) is nearly coplanar with the central NC$_3$ plane (dihedral angle = 3.4°), while the remaining two pyridyl rings have dihedral angles of 63.1 and 65.0°, respectively, with the NC$_3$ unit. The Zn−N and Zn−Cl bond lengths in **1** are typical.[9] The noncoordinating N(4) atom is 4.33 Å from the zinc center.

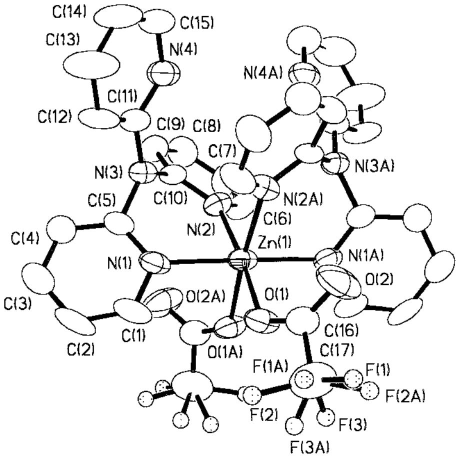

Figure 4. ORTEP diagram showing the structure of compound **2** with 50% thermal ellipsoids and the atom-labeling schemes.

The structure of compound **2** is shown in Figure 4. Compound **2** has a crystallographically imposed 2-fold rotation symmetry. There are two independent molecules in the asymmetric unit. The structures and bond lengths and angles for these two independent molecules are essentially identical. Therefore, only one of the independent molecules is shown here. The zinc center is six-coordinate with an octahedral geometry. Two 2,2′,2″-tpa ligands chelate to the zinc center in a fashion similar to that observed in compound **1**. Two trifluoroacetate ligands are coodinated to the zinc center as terminal ligands and in a cis geometry. The crystals of the trans geometric isomer of **2** were not obtained. The Zn−N bond lengths (2.156−2.182 Å) are much longer than those of compound **1** (2.057−2.058 Å), obviously resulting from the increased number of ligands in compound **2**. The Zn−O bond lengths are normal.[9] The noncoordinated nitrogen atom N(4) is 4.824 Å from the zinc center. The central NC$_3$ portion of the 2,2′,2″-tpa ligand in compound **2** is planar. One of the pyridyl rings (N(4)) is nearly coplanar with the NC$_3$ plane (dihedral angle = 7.3°), while the remaining two pyridyl rings have dihedral angles of 65.3 and 62.6°, respectively, with the NC$_3$ plane. There appears to be some $\pi-\pi$ stacking between the pyridyl rings of the two 2,2′,2″-tpa ligands, as indicated by the C(11)−N(2A) distance of 3.536 Å. Many examples of zinc(II) complexes with an octahedral geometry have been observed previously.[9a,10] In principle, 2,2′,2″-tpa can function not only as a bidentate chelating ligand but also as a tridentate chelating ligand where all three pyridyl groups bind to the same central atom. It is therefore interesting that only the bidentate bonding mode is observed in compound **1**, where the zinc center is only four-coordinate. The bidentate binding mode of 2,2′,2″-tpa in **2** could be explained by the coordination saturation around the zinc atom.

The structure of compound **3** is shown in Figure 5. Compound **3** has a crystallographically imposed inversion center of symmetry. There are four 2,2′,3″-tpa ligands in **3**. However, in contrast to 2,2′,2″-tpa, the 2,2′,3″-tpa ligands in **3** function as terminal ligands and bind to the zinc (II) center by the 3-pyridyl nitrogen atoms only. The steric interactions between the four 2,2′,3″-tpa ligands must be responsible for the terminal bonding mode. The two trifluoroacetate ligands are coordinated to the Zn(1) center as terminal ligands in a trans fashion, leading to the six-coordinate octahedral geometry of the zinc center. The two noncoordinating 2-pyridyl rings in the 2,2′,3″-tpa ligand have an orientation similar to that in the free ligand; i.e., the

---

(9) (a) Prince, R. H. In *Comprehensive Coordination Chemistry*; Wilkinson, G., Gillard, R. D., McCleverty, J. A., Eds.; Pergamon Press: New York, 1987; Vol. 5, Chapter 56.1. (b) Auf der Heyde, T. P. E. *Acta Crystallogr*, **1984**, *B40*, 582. (c) Kerr, M. C.; Preston, H. S.; Ammon, H. L.; Huheey, J. E.; Stewart, J. M. *J. Coord. Chem.* **1981**, *11*, 111. (d) Smith, H. W. *Acta Crystallogr.* **1975**, *B31*, 2701.

(10) Mikami-Kido, M.; Saito, Y. *Acta Crystallogr.* **1982**, *B38*, 452.

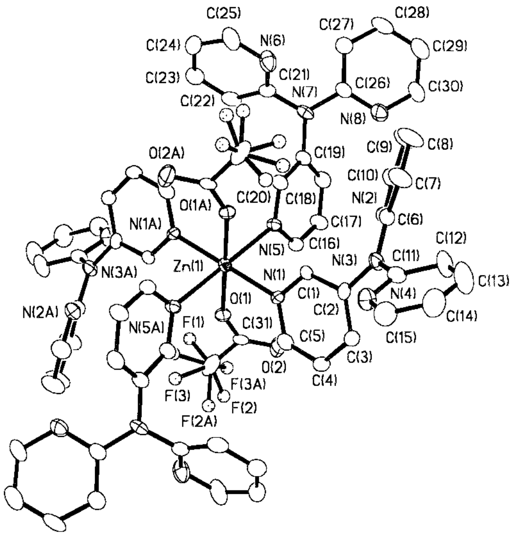

Figure 5. ORTEP diagram showing the structure of compound **3** with 50% thermal ellipsoids and the atom-labeling scheme.

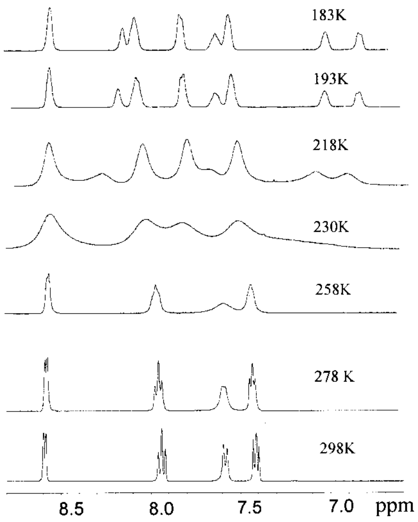

Figure 6. ^{1}H NMR spectra of compound **1** in CD_2Cl_2 at 183−298 K.

nitrogen atoms are oriented away from each other. Two structural isomers, trans and cis, are possible for compound **3**. However, only the trans isomer was observed for compound **3**, again attributable to steric interactions. The central NC_3 unit of 2,2′,3″-tpa in **3** is planar. The smallest dihedral angle between a pyridyl ring and the NC_3 plane is 12.3° (N(8)).

Fluxional Behavior of Compounds 1 and 2. In compound **1**, two of the 2-pyridyl rings in the 2,2′,2″-tpa ligand are chelated to the Zn(1) center in an approximately symmetric fashion, while the remaining 2-pyridyl ring is not coordinated. If compound **1** retains the same structure in solution, two sets of distinct chemical shifts due to the coordinate and noncoordinate 2-pyridyl rings should be observed in the ^{1}H NMR spectrum of compound **1**. However, the ^{1}H NMR spectrum of **1** at ambient temperature shows only one set of 2-pyridyl chemical shifts, indicative of the presence of some dynamic exchange in solution. To confirm this, we examined the ^{1}H NMR spectrum of **1** over the temperature range of 183−298 K using CD_2Cl_2 as the solvent. The variable-temperature NMR spectra of **1** are shown in Figure 6. At 183 K, two sets of 2-pyridyl chemical shifts in a 2:1 ratio assigned to the coordinate and noncoordinate pyridyl groups were observed, thus confirming that, at 183 K, the structure of compound **1** in solution is the same as that in the solid state. As the temperature increased, all chemical shifts became broad and coalesced at about 230 K, consistent with the presence of an exchange process between the coordinate and noncoordinate 2-pyridyl rings. At 298 K, only one set of 2-pyridyl chemical shifts were observed, attributable to a fast exchange at this temperature. The proposed exchange mechanism is shown in Scheme 2. The behavior of **1** in THF-d_8 is similar to that in CD_2Cl_2. Similar exchange phenomena involving tripod ligands such as HOC(2-Py)(1-methylimidazole)$_2$ have been reported previously.[11]

Scheme 2

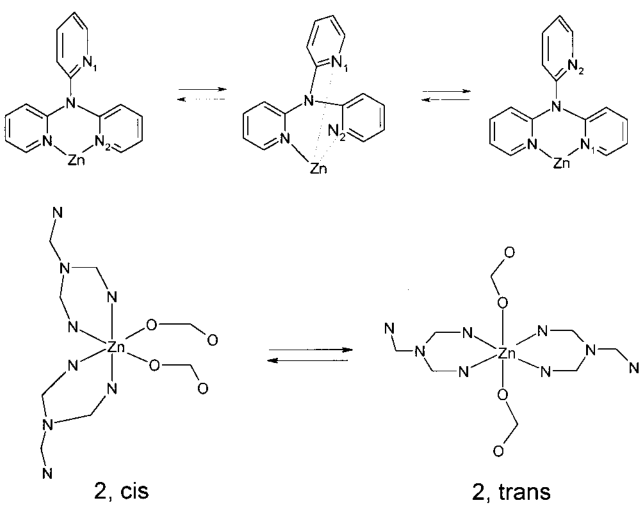

The observed structure for compound **2** in the solid state is the cis isomer where all three 2-pyridyl rings of 2,2′,2″-tpa are not equivalent: there are one noncoordinating 2-pyridyl and two coordinating 2-pyridyls, one in the basal plane and the other in the axial position. Therefore, if compound **2** retains the cis structure in solution, three sets of chemical shifts (12 peaks) in a 1:1:1 ratio due to the three distinct 2-pyridyl groups should be observed. The examination of compound **2** by ^{1}H NMR spectroscopy over the temperature range of 180−298 K using either THF-d_8 or CD_2Cl_2 as the solvent revealed that compound **2** is highly dynamic in solution. The behaviors of compound **2** in THF and dichloromethane are very similar. The variable-temperature ^{1}H NMR spectra of **2** in THF-d_8 are shown in Figure 7. At 298 K, only one set of chemical shifts due to 2-pyridyl are present, indicative of exchange. At 183 K, 13 peaks with nonequal intensities are observed, an indication that the cis isomer is not the only species present in solution. In the trans isomer of **2**, all coordinate 2-pyridyl rings are in the basal plane. Therefore, two sets of chemical shifts (8 peaks) in a 2:1 ratio due to the coordinate and noncoordinate 2-pyridyl rings should be present for the trans isomer. If cis and trans isomers coexist in solution, 20 peaks should be present in the ^{1}H NMR spectrum of **2**. Accidental peak overlaps could reduce the number of peaks observed, which we believe is the case for compound **2**; i.e., the observed 13 peaks with nonequal intensities are due to the coexistence of cis and trans isomers. To assign the chemical shifts to the corresponding isomers, we attempted 2D exchange NMR (EXSY) and COSY experiments at 183 K. However, due to the extensive peak overlaps, conclusive peak assignments were unsuccessful. Nevertheless, the NMR spectra shown in Figure 7 indicated that it is most

---

(11) (a) Canty, A. J.; Minchin, N. J.; Healy, P. C.; White, A. H. *J. Chem. Soc., Dalton Trans.* **1982**, 1795. (b) Byers, P. K.; Canty, A. J.; Minchin, N. J.; Patrick, J. M.; Skelton, B. W.; White, A. H. *J. Chem. Soc., Dalton Trans.* **1985**, 1183.

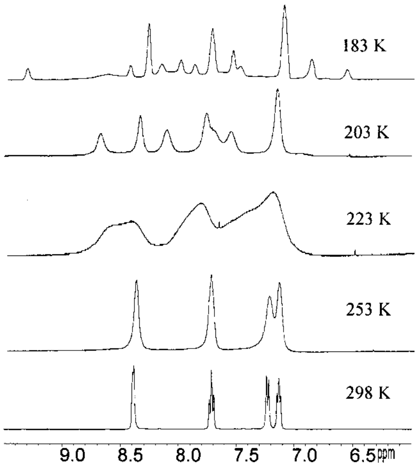

Figure 7. ^{1}H NMR spectra of compound **2** in THF-d_8 at 183−298 K.

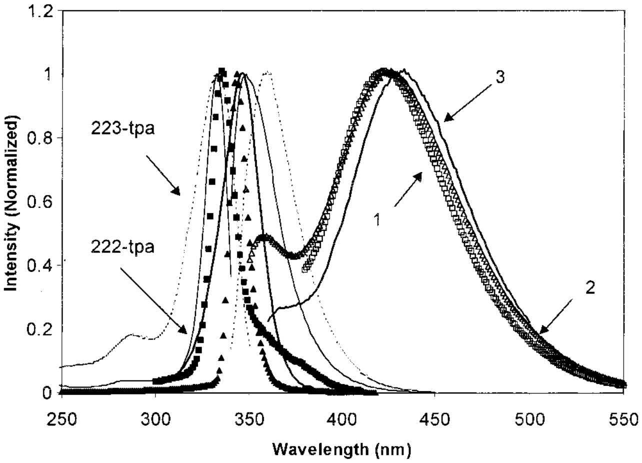

Figure 8. THF solution excitation and emission spectra of 2,2′,2″-tpa (thin solid lines), 2,2′,3″-tpa (dashed lines), compound **1** (solid squares, excitation; empty squares, emission), **2** (solid triangles, excitation; empty triangles, emission), and **3** (dark solid lines).

likely that compound **2** exists as both cis and trans isomers in solution. The dynamic behavior of **2** can be attributed to both isomer interconversion and exchange of coordinate and noncoordinate 2-pyridyl rings.

The four 2,2′,3″-tpa ligands in the trans isomer of compound **3** are essentially equivalent. Therefore, only one set of chemical shifts due to 2,2′,3″-tpa should be observed in the ^{1}H NMR spectrum of **3**, if **3** exists as the trans isomer only. Indeed, variable-temperature ^{1}H NMR spectra for compound **3** in THF-d_8 or CD_2Cl_2 in the temperature range of 183−298 K show only one set of chemical shifts due to the 2,2′,3″-tpa ligand which do not change with temperature. We therefore concluded that compound **3** exists as the trans isomer only and is not fluxional in solution. The nonfluxional behavior of **3** in solution, in contrast to those of **1** and **2** can be attributed to the fact that there are four 2,2′,3″-tpa ligands in **3**, which makes the molecule very crowded, thus favoring the sterically less demanding trans isomer.

Luminescent Properties of Compounds 1−3. 2,2′,2″-tpa and 2,2′,3″-tpa ligands have no emission in the visible region. In solution, these two ligands have sharp emission bands at λ_{max} = 347 and 360 nm, respectively (Figure 8). When these ligands were bound to a zinc center, blue luminescence was observed. Because $ZnCl_2$ and $Zn(O_2CCF_3)_2$ are not luminescent, the observed luminescence of the complexes is attributed to the coordinate 2,2′,2″-tpa and 2,2′,3″-tpa ligands. As shown in Figure 8, in contrast to the free ligands, compounds **1**−**3** in solution each have a broad emission band (bandwidth at half-height = 80−90 nm) with λ_{max} = 422, 426, and 432 nm, respectively. Previously reported 2,2′-dipyridylamine Zn(II) complexes emit mostly at λ_{max} <400 nm in solution and in the solid state.[7] The replacement of a proton on the amino group in 2,2′-dipyridylamine by a pyridyl group apparently resulted in a decrease of the HOMO−LUMO energy gap of the 2,2′,2″-tpa and 2,2′,3″-tpa ligand in complexes **1**−**3**. To understand the origin of the red shift of the emission energy from the free ligand to the complex, we performed ab initio calculations for the free ligand, 2,2′,2″-tpa, and compound **1** at the restricted Hartree−Fock (RHF) level using a standard split-valence polarized (6-31G*) basis set for the free ligand and an unpolarized (6-31G*) basis set for the zinc atom and employing the Gaussian 98 suite of programs.[12] The geometric parameters were obtained from crystal structural data. In Figure 9 are plotted the energies of the highest occupied molecular orbitals (HOMO's) and lowest unoccupied molecular orbitals (LUMO's) for the free ligand and compound **1**, together with the surfaces on which these orbitals attain values of ±0.05 au. As one may see, the HOMO of the free ligand (which has a C_3 symmetry) is a π orbital with contributions from all three 2-pyridyl rings and a substantial contribution from the lone pair of the amino nitrogen atom. The HOMO of the complex is also a π orbital localized on the noncoordinating pyridyl ring (N(4)) and the lone pair of the amino nitrogen atom, owing to the low symmetry (C_1). However, the nodal structure of the HOMO of the ligand is not compatible with that of the complex. The energy of the HOMO level of the complex is much lower than that of the free ligand. The LUMO of the free ligand is a π* orbital with contributions from all three pyridyl rings, while the LUMO of the complex is a π* orbital consisting of mostly atomic orbitals from one of the coordinated pyridyl rings. There is essentially no contribution from the amino nitrogen in the LUMO's of the free ligand and the complex. The observed emission of the free ligand and the complex can be therefore attributed to the transition between π (HOMO) and π* (LUMO) levels. The LUMO energy level of the complex is again much lower than that of the free ligand. The decrease in the energies of both HOMO and LUMO levels in the complex relative to those of the free ligand is caused by the coordination of the pyridyl rings to the zinc center, which makes the nitrogen atoms of the pyridyl rings more electronegative, thus lowering the energy of the molecular orbitals. The net effect is that the HOMO−LUMO energy gap of the complex is smaller than that of the free ligand, as shown in Figure 9. Consequently, the emission energy of the complex has a red shift in comparison to that of the free ligand. Due to the exaggerated gap in Hartree−Fock calculations, the HOMO−LUMO energy gap difference does not at all correspond to the experimental values. However, the qualitative trend is retained.

---

(12) Frisch, M. J.; Trucks, G. W.; Schlegel, H. B.; Scuseria, G. E.; Robb, M. A.; Cheeseman, J. R.; Zakrzewski, V. G.; Montgomery, J. A., Jr.; Stratmann, R. E.; Burant, J. C.; Dapprich, S.; Millam, J. M.; Daniels, A. D.; Kudin, K. N.; Strain, M. C.; Farkas, O.; Tomasi, J.; Barone, V.; Cossi, M.; Cammi, R.; Mennucci, B.; Pomelli, C.; Adamo, C.; Clifford, S.; Ochterski, J.; Petersson, G. A.; Ayala, P. Y.; Cui, Q.; Morokuma, K.; Malick, D. K.; Rabuck, A. D.; Raghavachari, K.; Foresman, J. B.; Cioslowski, J.; Ortiz, J. V.; Stefanov, B. B.; Liu, G.; Liashenko, A.; Piskorz, P.; Komaromi, I.; Gomperts, R.; Martin, R. L. D.; Fox, J.; Keith, T.; Al-Laham, M. A.; Peng, C. Y.; Nanayakkara, A.; Gonzalez, C.; Challacombe, M.; Gill, P. M. W.; Johnson, B.; Chen, W.; Wong, M. W.; Andres, J. L.; Gonzalez, C.; Head-Gordon, M.; Replogle, E. S.; Pople, J. A. *Gaussian 98*, Revision A.6; Gaussian, Inc.: Pittsburgh, PA, 1998.

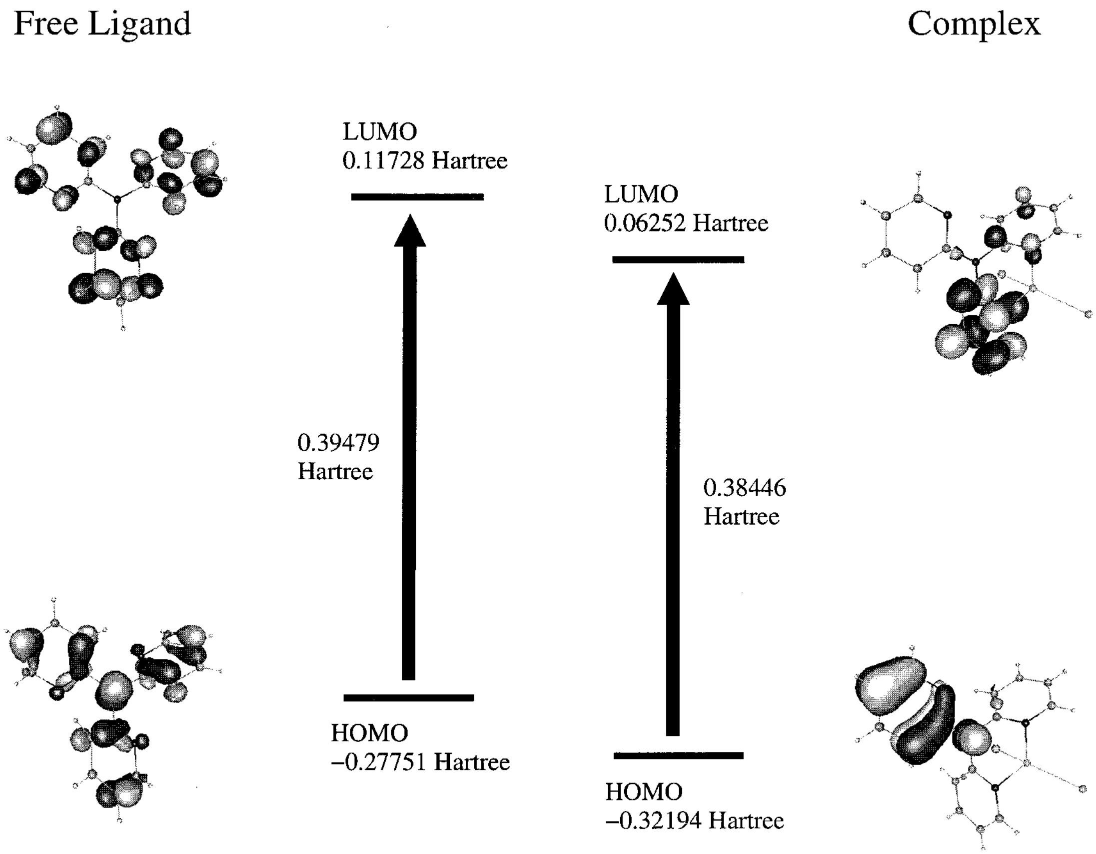

Figure 9. HOMO and LUMO orbitals of 2,2′,2″-tpa and compound **1**.

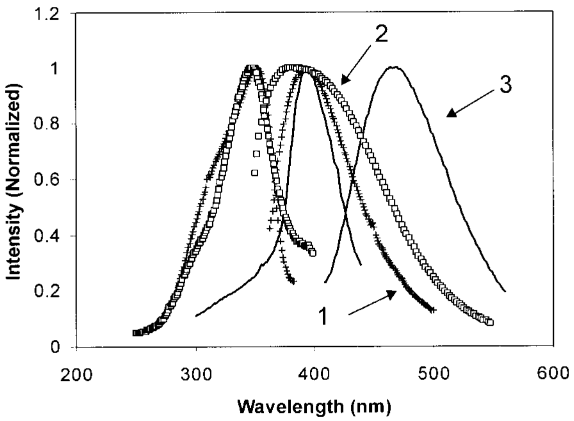

Figure 10. Excitation and emission spectra in the solid state of **1** (crosses), **2** (empty squares), and **3** (solid lines).

In addition to red-shifting the emission energy, the formation of complexes also significantly enhances the emission efficiencies of the ligands. The quantum yields for 2,2′,2″-tpa and 2,2′,3″-tpa were determined to be 0.026 and 0.024, respectively, relative to that of 9,10-diphenylanthracene. In contrast, the quantum yields for compounds **1**−**3** were determined to be 0.054, 0.22, and 0.10, respectively. The chelating mode of the ligand and the absence of heavy atoms such as chlorine are believed to be responsible for the relatively high quantum yield of compound **2**. A similar enhancement of quantum yield by coordination has been observed previously.[4,13] The excitation and emission spectra of compounds **1**−**3** in the solid state are shown in Figure 10. Despite the similarity of their emission bands in solution, the emission bands of the three compounds in the solid state are quite different. Compound **1** has a relatively narrow emission band with $\lambda_{max} = 395$ nm (bandwidth at half-height = 77 nm), while compound **2** has a very broad emission band (bandwidth at half-height = 120 nm) with $\lambda_{max} = 385$ nm. Although the emission maxima of **1** and **2** in the solid state are no longer in the blue region, the emission bands of both compounds cover much of the blue region, giving the observed blue luminescence. Compound **3** has a broad emission band (bandwidth at half-height = 100 nm) with $\lambda_{max} = 470$ nm in the solid state, giving the appearance of a whitish-blue luminescence. The deviation of the solid-state emission spectra from those of solutions is likely caused by crystal packing differences of compounds **1**−**3** in the solid state. It is however surprising that compounds **1** and **2** have a blue shift while compound **3** has a red shift from solution to the solid state. In the crystal lattice of **1**, there are $\pi-\pi$ stackings between the noncoordinating pyridyl rings of neighboring molecules, with the shortest atomic separation distance being 3.885 Å. There is however no intermolecular stacking in the crystal lattice of **2**. In the crystal lattice of **3**, there is an extensive $\pi-\pi$ stacking between the coordinate 3-pyridyl ring and one of the noncoordinate 2-pyridyl rings, with the shortest atomic separation distance being 3.582 Å. The observed emission energy red shift of **3** from solution to the solid state could be caused by the $\pi-\pi$ interactions between 2-pyridyl and 3-pyridyl rings. Further research is required to better understand this phenomenon.

Conclusion

We demonstrated here that 2,2′,2″-tpa and 2,2′,3″-tpa ligands form a variety of Zn(II) complexes which have interesting structural features and display rare blue luminescence. The

---

(13) (a) *Photochemistry and Photophysics of Coordination Compounds*; Yersin, H., Vogler, A., Eds.; Springer-Verlag: Berlin, 1987. (b) *Concepts of Inorganic Photochemistry*; Adamson, A. W., Fleischauer, P. D., Eds.; John Wiley & Sons: New York, 1975.

coordination of the 2,2′,2′′-tpa and 2,2′,3′′-tpa ligands to a Zn(II) center causes a shift of emission energy from UV to blue and an increase in emission efficiency. Zn(II) complexes of 2,2′,2′′-tpa are fluxional in solution owing to the intramolecular exchange of coordinate and noncoordinate 2-pyridyl rings. There is a significant difference between the emission spectra of compounds **1**−**3** in solution and in the solid state, the cause of which is yet to be understood. Compounds **1**−**3** have the potential to be used as blue emitters in electroluminescent devices. Efforts are being taken by our group to investigate the electroluminescent properties of compounds **1**−**3** and the results will be reported elsewhere.

Acknowledgment. We thank the Natural Sciences and Engineering Council of Canada and the Xerox Research Foundation for financial support.

Supporting Information Available: Lisings of X-ray experimental details, atomic coordinates, thermal parameters, and bond distances and angles. This material is available free of charge via the Internet at http://pubs.acs.org.

IC991436M